PNAS
www.pnas.org

Supplementary Information for

Repression of human and mouse brain inflammaging transcriptome by broad gene-body histone hyperacetylation

Hao Cheng[a.b.1], Hongwen Xuan[a.b.1], Christopher D. Green[a], Yixing Han[a], Na Sun[a], Hongjie Shen[c.d.e], Joseph McDermott[a], David A. Bennett[f], Fei Lan[c.d.e] and Jing-Dong J. Han[a.2]

Jing-Dong J. Han
Email: jdhan@picb.ac.cn

This PDF file includes:

www.pnas.org/cgi/doi/10.1073/pnas.1800656115

Supplementary Information Text

Supplemental Experimental Procedures.

Human samples

Human brain prefrontal cortex materials were obtained from Chinese Brain Bank Center (CBBC) in Wu Han, China, Religious Order Study (ROS) and Rush Memory and Aging Project (MAP) at the RUSH Alzheimer's Disease Center, and National Institute of Child Health and Human Development (NICHD) Brain and Tissue Bank for Development Disorders at the University of Maryland. Baltimore, MD, USA. Informed consent was obtained for the use of the human tissues. For each pooled group, equal weight of PFC samples from different individuals within the same age range were mixed together for next step use. Details of samples are in Supplementary Table 1.

In vivo animal studies

C57BL/6 mice were cultured in Shanghai Model Organisms Center, Inc. with standard condition proved by The Association for Assessment and Accreditation of Laboratory Animal Care International (AAALAC), drug treatment, Morris water maze and brain tissue collection were also done by here. For drug treatment, mice were treated three times a week with DMSO (Sigma, Cat. # D2650) or SAHA (Cayman, Cat. # 10009929), which was diluted to 5% in normal saline, for 3 months by using intragastric administration (Table S3). In both batch 1 and 2 of these experiments studying aging effects and their attenuation by SAHA, female mice were used, while in the experiment studying SAHA dosage, male mice were used, which showed a similar response as female mice in the other experiments.

Brain RNA extraction and library preparation

50 mg human tissues or 20 mg mouse tissues were lysed in TRIzol (ThermoFisher, Cat. # 15596026) using a TissueRuptor (QIAgen, Cat. # 9001271). Total RNA was extracted according to TRIzol standard procedures. All samples with the RNA integrity number (RIN, measured by Agilent RNA 6000 Nano Kit, Cat. # 5067-1511) >5 in human or >8 in mouse were used to construct sequencing libraries using Illumina standard protocols. Human brain R group polyA plus 50 bp single-end reads were generated by Illumina Hi-Seq2000. Mouse brain ribo minus 125 bp (batch 1 and 3) and 150 bp (batch 2) pair-end reads were generated by Illumina Hi-Seq2500 and Hi-Seq X Ten.

Brain ChIP and library preparation

150 mg human tissues or 30 mg mouse tissues were homogenize and crosslinked, 10 μ~1mg lysis buffer with cOmplete™, Mini, EDTA-free Protease Inhibitor Cocktail (Sigma, Cat. # 4693159001) were added. Samples were sonicated by Bioruptor® Plus sonication device (diagenode, Cat. # B01020001) for 40 min at high power (30 s on/30 s off). After overnight incubate with 2.5 μl Rabbit polyclonal anti-H3K27ac (Abcam, Cat. # ab4729), 40 μl Dynabeads™ Protein G (ThermoFisher, Cat. # 10004D) were added to each sample for 2 h. Harvested beads were incubated with proteinase K (ThermoFisher, Cat. # AM2546) and RNase A (ThermoFisher, Cat. # EN0531) overnight. DNA fragment

were extracted by MinElute PCR Purification Kit (QIAGEN, Cat. # 28006). ChIP libraries were constructed using Illumina standard protocols. Human brain 50 bp (R group) and 100 bp (N group) single-end reads were generated by Illumina Hi-Seq2000. Mouse brain 125 bp (batch 1) and 150 bp (batch 2) pair-end reads were generated by Illumina Hi-Seq2500 and Hi-Seq X Ten, 50 bp (batch 3) single-end reads were generated by Illumina Hi-Seq2000.

Data process

DAVID (v6.8) (1, 2) was used to do functional annotations, Benjamini adjust p-value are shown. Peaks from ChIP-seq data were called through MACS2 (v2.1.0) callpeak (3). Super enhancers were identified by ROSE (4, 5).

Functional gene association networks

The functional gene association networks were generated by STRING (v10.5) (6) with default parameters (minimum combined confidence larger than 0.4). Inflammatory response (GO:0006954, download date 2018-03-23) gene lists for human was downloaded from the Gene Ontology (7, 8). Cytoscape (v3.6.0) was used to visualize networks.

DEGs prediction with generalized linear model (GLM)

The GLMs were derived using R with parameter family=binomial(link='logit'). For each dataset, 90% genes are used as training data and the remaining 10% genes are used as testing data. Input features include: acetylation density on upstream of TSS (-2kbp to TSS), gene body, gene downstream (TTS to +2kbp), closest typical or super enhancer and $\log_2$ fold change between old/young or SAHA/control. 10-fold cross-validation using 10 non-overlapping gene groups were performed for each dataset with cv.glm function and adjusted cross-validation estimate delta were shown. ROC is generated with the remaining 10% testing data by R to avoid overfitting the model.

Morris Water Maze

The method of Morris water maze was adapted from previous published method (9). Experiment was done during last week with treatment. For 5 days hidden platform training, latency were measured as the time of each mice located to the platform, failed mice recorded as 60 seconds. For final probe trials, platform was removed, platform crosses were measured as the number of each mice cross the previously platformed area. Results are visualized by GraphPad Prism (v6.01).

Figure S1

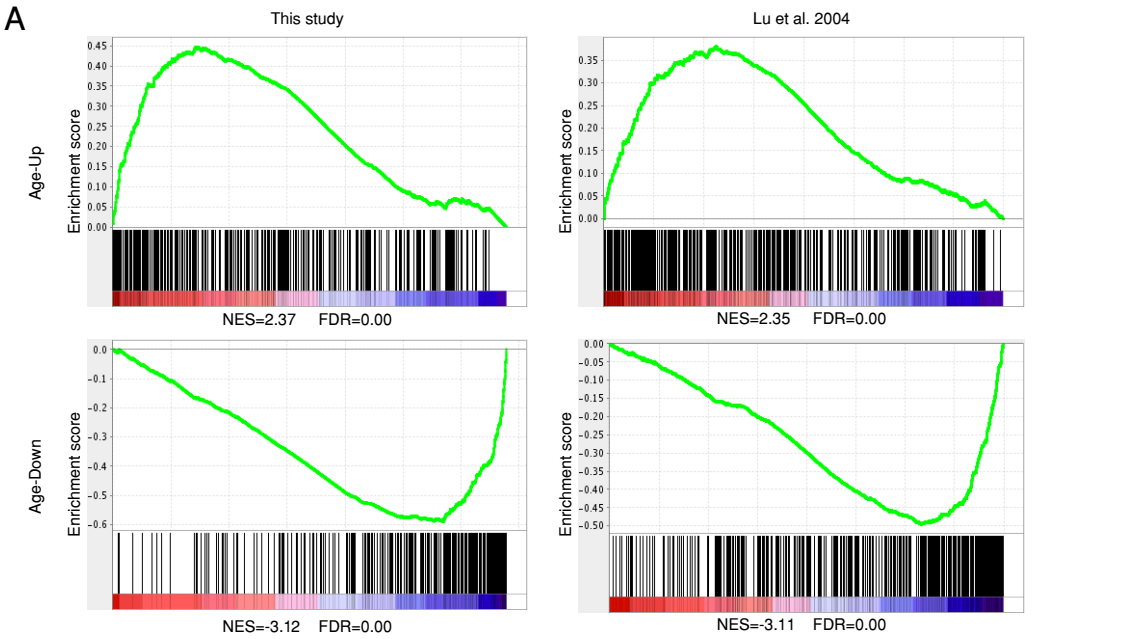
A
This study
Lu et al. 2004
Age-Up
Age-Down
Enrichment score
NES=2.37 FDR=0.00
NES=2.35 FDR=0.00
NES=-3.12 FDR=0.00
NES=-3.11 FDR=0.00

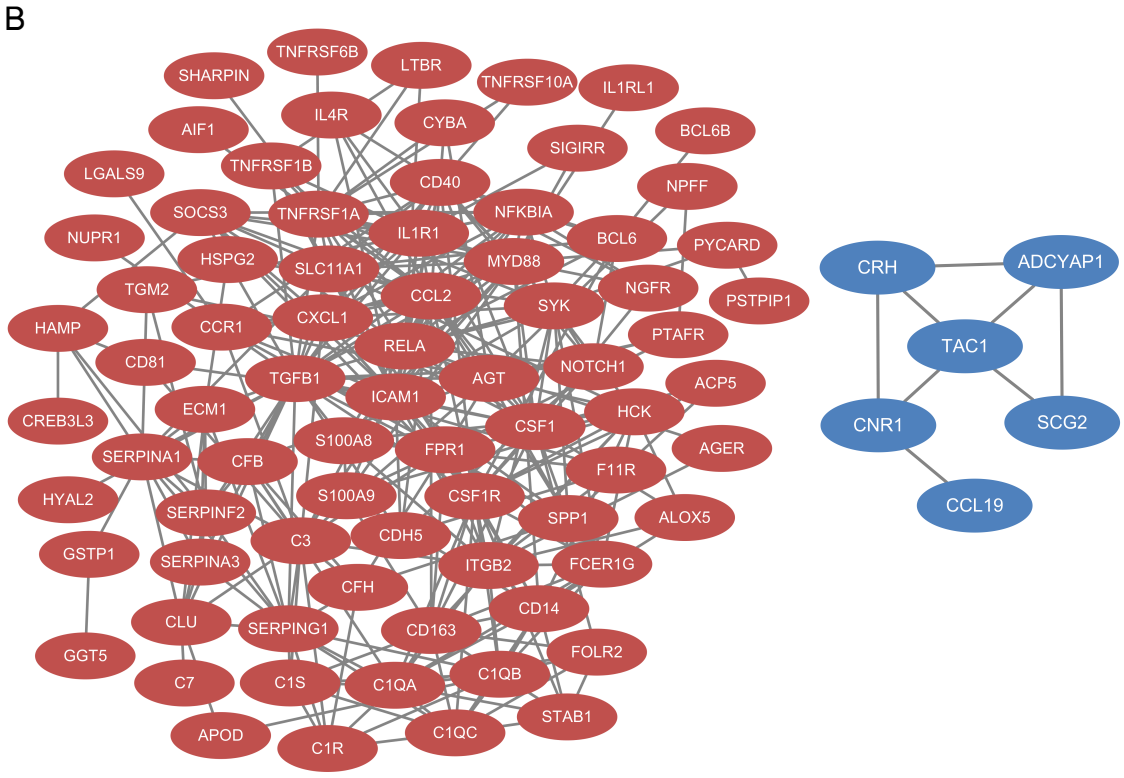
B
TNFRSF6B
LTBR
SHARPIN
TNFRSF10A
IL1RL1
IL4R
CYBA
AIF1
BCL6B
SIGIRR
TNFRSF1B
LGALS9
CD40
NPFF
SOCS3
TNFRSF1A
NFKBIA
NUPR1
IL1R1
BCL6
PYCARD
HSPG2
SLC11A1
MYD88
TGM2
CCL2
NGFR
PSTPIP1
SYK
HAMP
CCR1
CXCL1
PTAFR
RELA
CD81
NOTCH1
TGFB1
AGT
ACP5
ICAM1
ECM1
HCK
CREB3L3
CSF1
S100A8
SERPINA1
FPR1
AGER
CFB
F11R
HYAL2
S100A9
CSF1R
SERPINF2
SPP1
ALOX5
C3
CDH5
GSTP1
SERPINA3
ITGB2
FCER1G
CFH
CD14
CLU
SERPING1
CD163
GGT5
FOLR2
C7
C1S
C1QA
C1QB
STAB1
APOD
C1R
C1QC
CRH
ADCYAP1
TAC1
CNR1
SCG2
CCL19

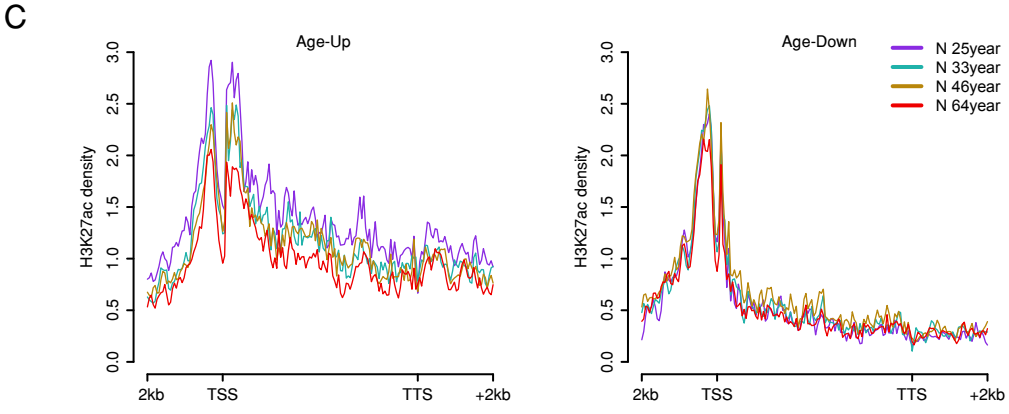
C
Age-Up
Age-Down
H3K27ac density
N 25year
N 33year
N 46year
N 64year
2kb
TSS
TTS
+2kb

Fig. S1. Human brain RNA-seq data in this study has significant agreement with published microarray data.
(A) Comparison between DEGs of human brain RNA-seq data in this study and in Lu et al. 2004 microarray datasets by GSEA, rank lists are all genes sorted by Spearman rank correlation coefficients (RCC) to age in our RNA-seq data or in Lu et al. 2004 microarray datasets.
(B) Functional gene association networks of the inflammatory response genes among Age-Up (red nodes) or Age-Down (blue nodes) genes in human brain.
(C) N group H3K27ac profiles on Age-Up and Age-Down genes from intersections between Lu et al. 2004 microarray data and our RNA-seq data.

Figure S2

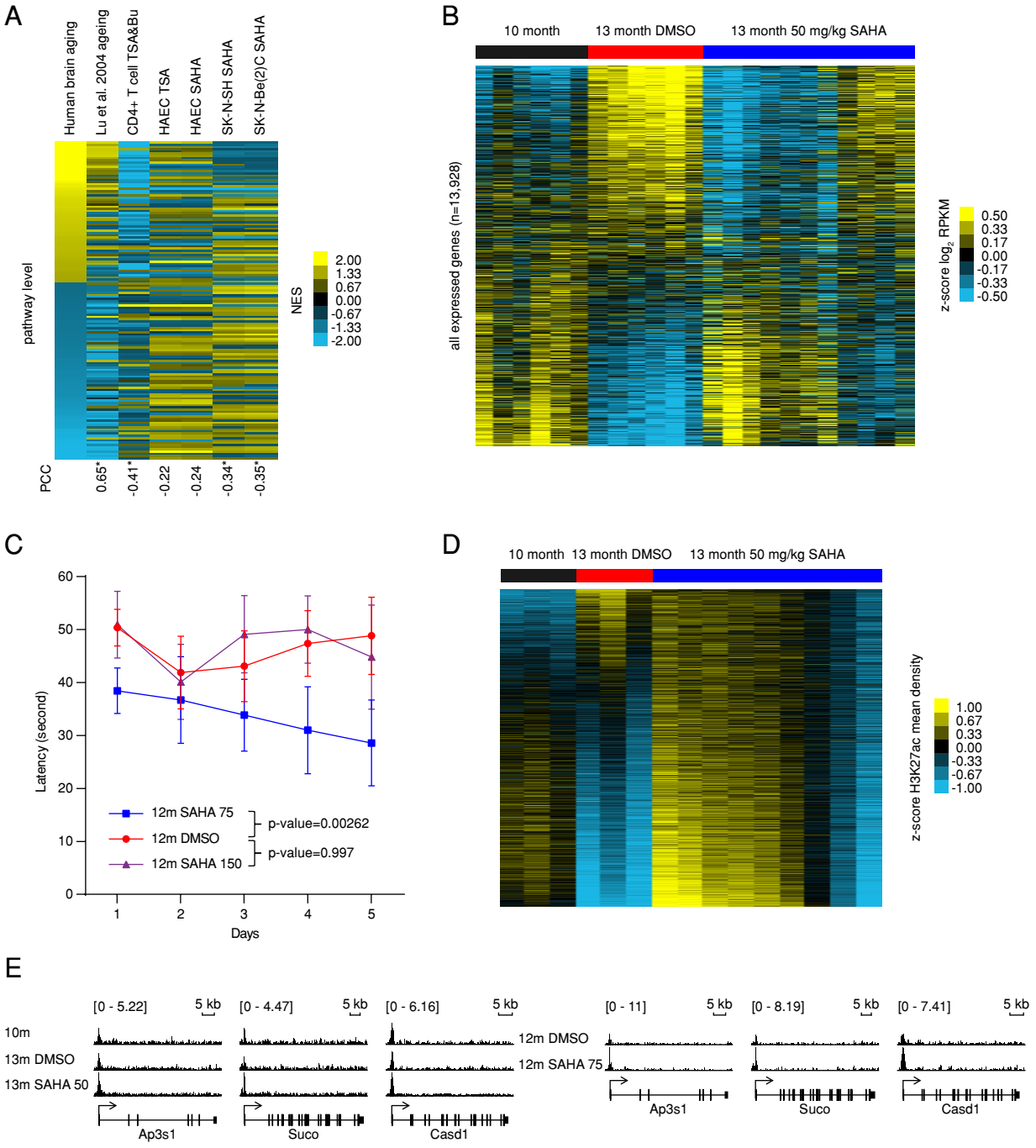
A
Human brain aging
Lu et al. 2004 ageing
CD4+ T cell TSA&Bu
HAEC TSA
HAEC SAHA
SK-N-SH SAHA
SK-N-Be(2)C SAHA
pathway level
NES
2.00
1.33
0.67
0.00
-0.67
-1.33
-2.00
PCC
0.65*
-0.41*
-0.22
-0.24
-0.34*
-0.35*
B
10 month
13 month DMSO
13 month 50 mg/kg SAHA
all expressed genes (n=13,928)
z-score log2 RPKM
0.50
0.33
0.17
0.00
-0.17
-0.33
-0.50
C
Latency (second)
Days
12m SAHA 75
12m DMSO
12m SAHA 150
p-value=0.00262
p-value=0.997
D
10 month
13 month DMSO
13 month 50 mg/kg SAHA
z-score H3K27ac mean density
1.00
0.67
0.33
0.00
-0.33
-0.67
-1.00
E
[0 - 5.22]
5 kb
[0 - 4.47]
[0 - 6.16]
[0 - 11]
[0 - 8.19]
[0 - 7.41]
10m
13m DMSO
13m SAHA 50
12m DMSO
12m SAHA 75
Ap3s1
Suco
Casd1

Fig. S2. HDAC inhibitors reverse age-related phenotype.
(A) KEGG pathways enriched in the top (positive NES) or bottom (negative NES) of the gene lists ranked by human brain age-dependent genes (sorted by their RCC to age) and HDACi induced DEGs (sorted by fold changes in HDACi vs. vehicle control samples) in different datasets. Yellow or blue color in the heatmap indicates a GSEA NES score for the terms enriched in the first column (nominal p-value< 0.05).
(B) Heatmap of $\log_2$ RPKM from all expressed genes with z-score normalization for individual mice, genes are ordered by average fold change between DMSO-treated 13-month and 10-month old mice.
(C) Latency comparison in the water maze test for 2 months and 3 weeks 75 or 150 mg/kg SAHA and DMSO treated 12-month old mice, mean value and SEM are shown on curves, KS test p-values between the SAHA and DMSO treated groups are shown above the point.
(D) Heatmap of from TSS – 2 kb to TTS + 2 kb of mouse brain Age-Up and Age-Down genes with z-score normalization for individual mice, genes are ordered by average fold change between DMSO-treated 13-month and 10-month old mice.
(E) Merged IGV views of H3K27ac profiles on exemplary Age-Down genes.

Figure S3

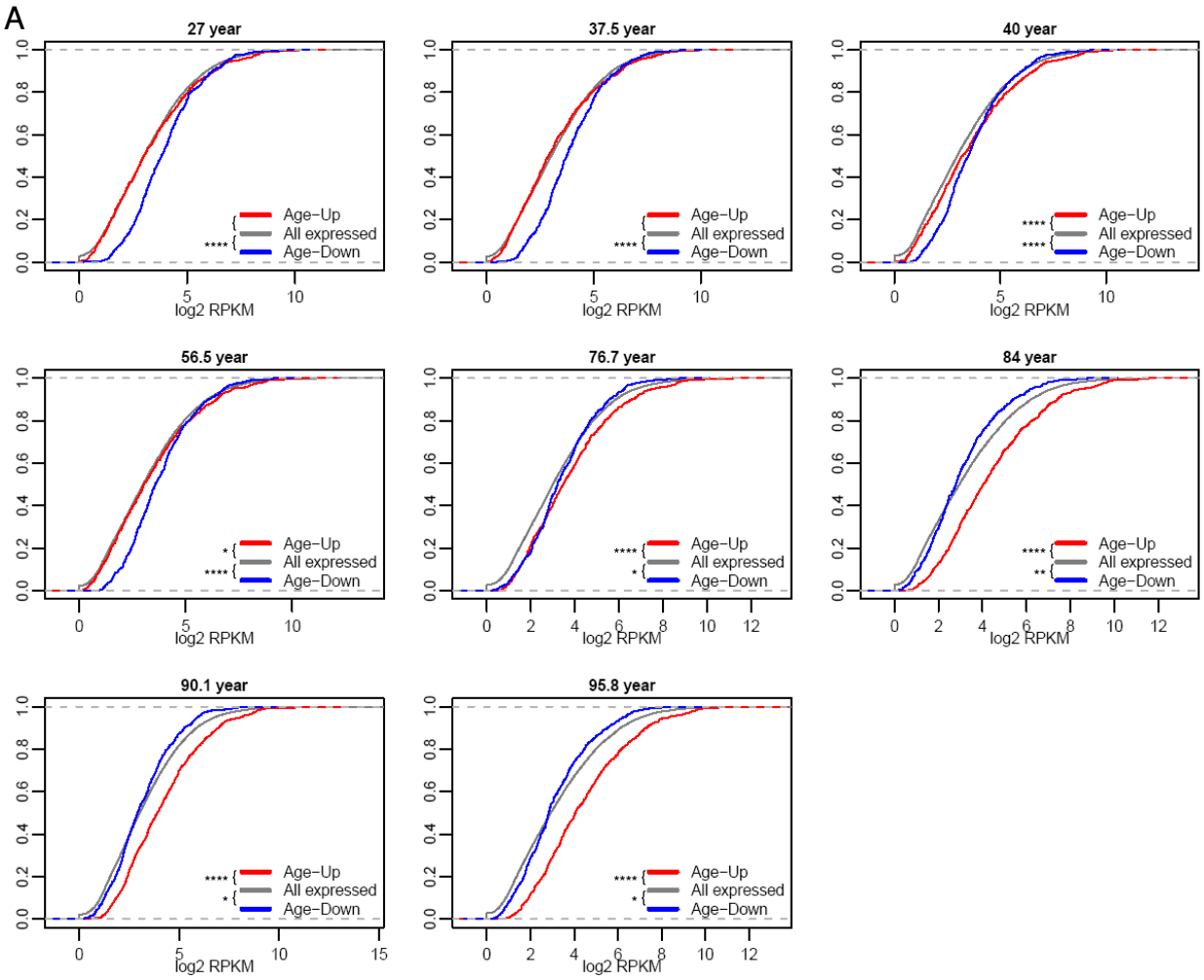
A
27 year
37.5 year
40 year
56.5 year
76.7 year
84 year
90.1 year
95.8 year
Age−Up
All expressed
Age−Down
log2 RPKM

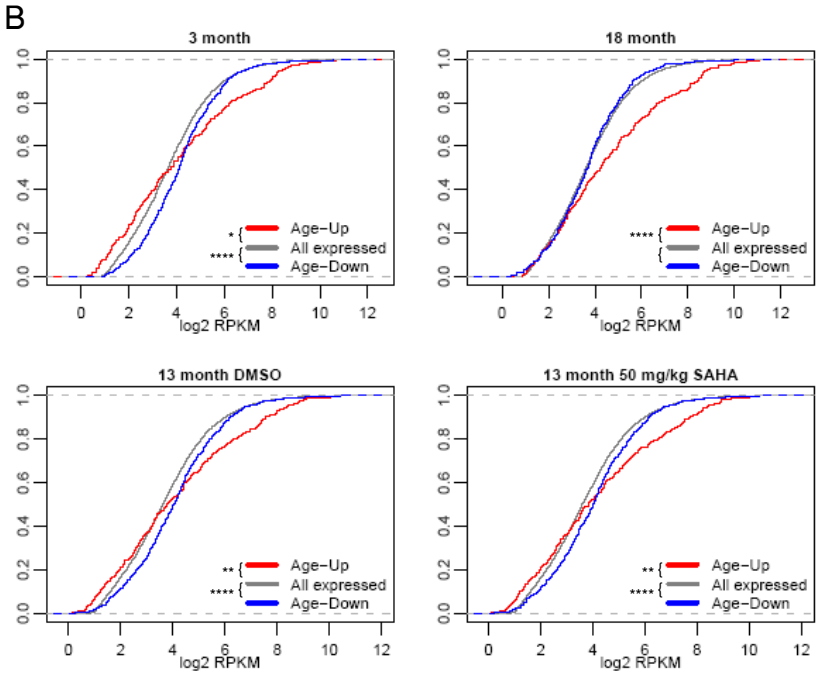
B
3 month
18 month
13 month DMSO
13 month 50 mg/kg SAHA
Age−Up
All expressed
Age−Down
log2 RPKM

Fig. S3. Age-Up genes are overexpressed in aged brains and attenuated by HDAC inhibition.
(A) Empirical cumulative distribution for $\log_2$ RPKM of Age-Up, Age-Down and all expressed genes in human brain, two-tail Student's t-test is used between each group. p-value < 0.05, 0.01, 0.001 and 0.0001 are marked as "*", "**", "***" and "****".
(B) Empirical cumulative distribution for $\log_2$ RPKM of Age-Up, Age-Down and all expressed genes in mouse brain, two-tail Student's t-test is used between each group. p-value < 0.05, 0.01, 0.001 and 0.0001 are marked as "*", "**", "***" and "****".

Figure S4

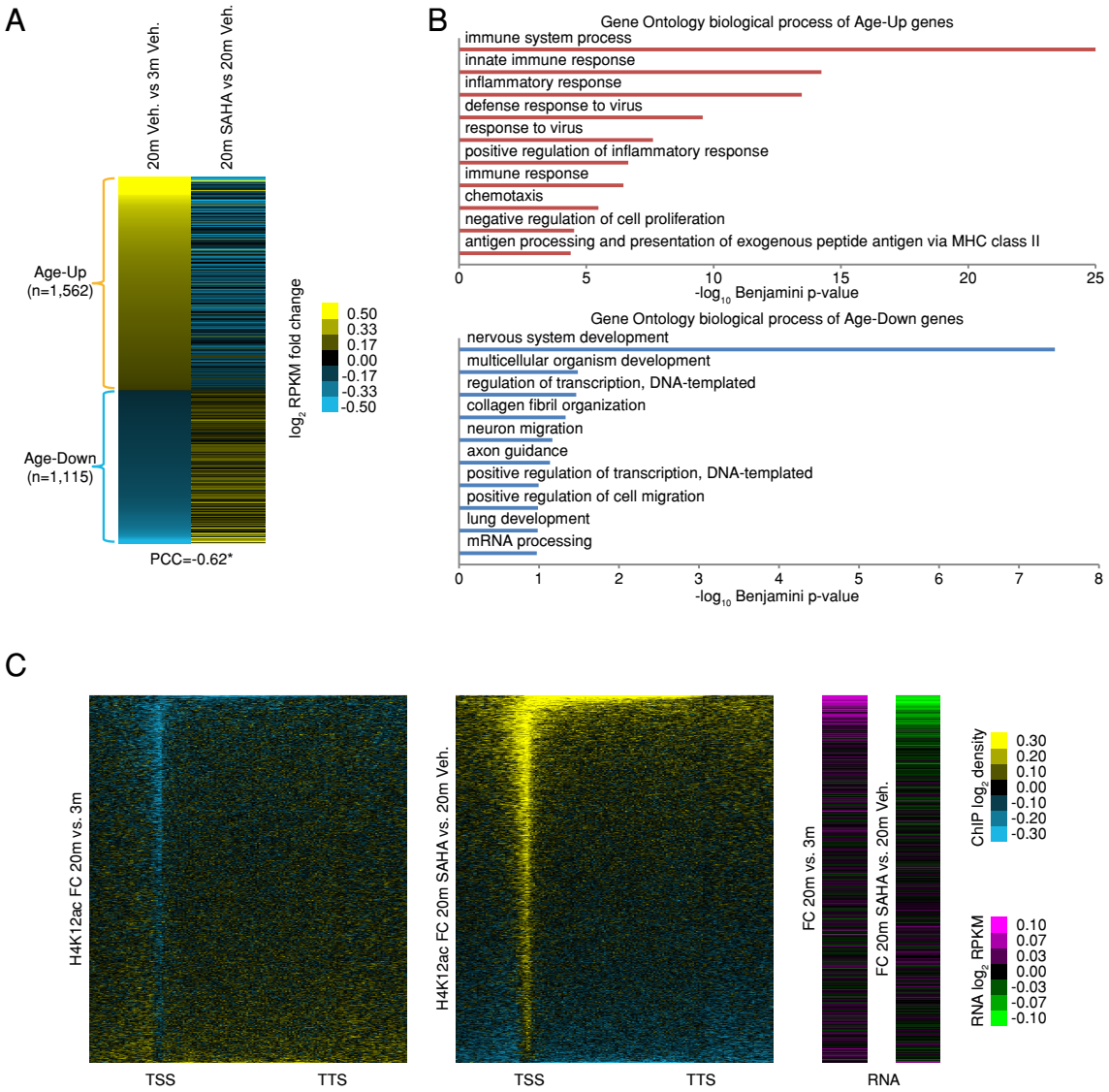
A
20m Veh. vs 3m Veh.
20m SAHA vs 20m Veh.
Age-Up
(n=1,562)
Age-Down
(n=1,115)
PCC=-0.62*
log2 RPKM fold change
0.50
0.33
0.17
0.00
-0.17
-0.33
-0.50
B
Gene Ontology biological process of Age-Up genes
immune system process
innate immune response
inflammatory response
defense response to virus
response to virus
positive regulation of inflammatory response
immune response
chemotaxis
negative regulation of cell proliferation
antigen processing and presentation of exogenous peptide antigen via MHC class II
0
5
10
15
20
25
-log10 Benjamini p-value
Gene Ontology biological process of Age-Down genes
nervous system development
multicellular organism development
regulation of transcription, DNA-templated
collagen fibril organization
neuron migration
axon guidance
positive regulation of transcription, DNA-templated
positive regulation of cell migration
lung development
mRNA processing
0
1
2
3
4
5
6
7
8
-log10 Benjamini p-value
C
H4K12ac FC 20m vs. 3m
TSS
TTS
H4K12ac FC 20m SAHA vs. 20m Veh.
TSS
TTS
FC 20m vs. 3m
FC 20m SAHA vs. 20m Veh.
RNA
ChIP log2 density
0.30
0.20
0.10
0.00
-0.10
-0.20
-0.30
RNA log2 RPKM
0.10
0.07
0.03
0.00
-0.03
-0.07
-0.10

Fig. S4. H4K12ac has a similar genome-wide pattern as H3K27ac during aging or under HDACi treatment.
(A) SAHA attenuates age dependent transcriptome changes in mouse CA1 hippocampal subregion. The mouse CA1 hippocampal subregion age dependent genes are sorted by their $\log_2$ fold change of expression between old (20-month) and young (3-month) mice (first column) with vehicle treatment (Veh.), then compared with those under 2 mg SAHA intake per day for 4 weeks (second column). Yellow/blue color in the first column indicates Age-Up/Down genes. The second column shows SAHA effects for the same genes. * indicates p-value of PCC<0.0001.
(B) Top 10 enriched GO biological process terms among mouse CA1 hippocampal subregion Age-Up and Age-Down genes determined by DAVID.
(C) Heatmaps of $\log_2$ fold changes of average H4K12 acetylation and expression in 20m Veh. vs. 3m Veh., 20m SAHA vs. Veh. treatment. Genes are ranked by average ChIP signal from upstream 2kb to downstream 2kb in 20m SAHA vs. Veh. treatment from high to low.

Figure S5

A

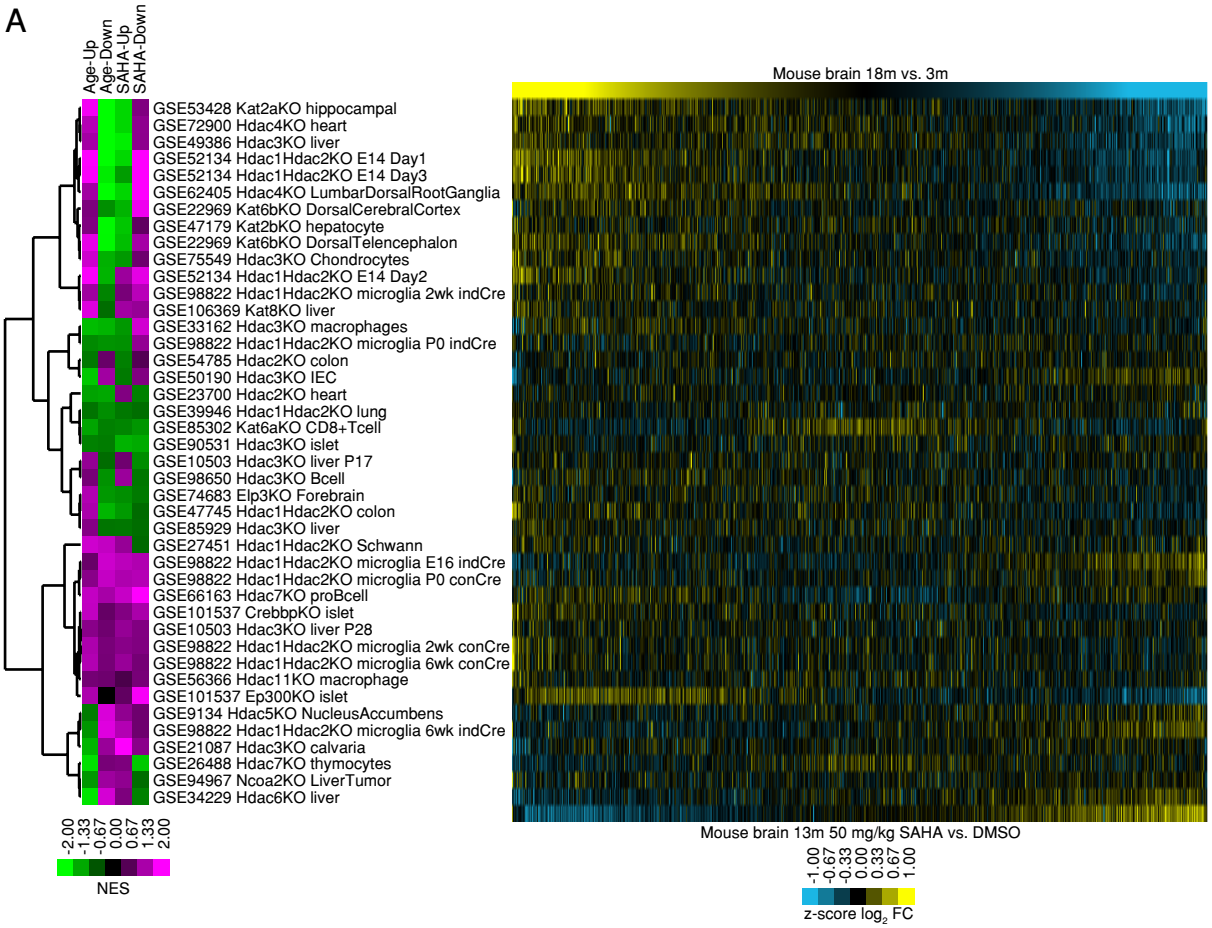
Age-Up
Age-Down
SAHA-Up
SAHA-Down
GSE53428 Kat2aKO hippocampal
GSE72900 Hdac4KO heart
GSE49386 Hdac3KO liver
GSE52134 Hdac1Hdac2KO E14 Day1
GSE52134 Hdac1Hdac2KO E14 Day3
GSE62405 Hdac4KO LumbarDorsalRootGanglia
GSE22969 Kat6bKO DorsalCerebralCortex
GSE47179 Kat2bKO hepatocyte
GSE22969 Kat6bKO DorsalTelencephalon
GSE75549 Hdac3KO Chondrocytes
GSE52134 Hdac1Hdac2KO E14 Day2
GSE98822 Hdac1Hdac2KO microglia 2wk indCre
GSE106369 Kat8KO liver
GSE33162 Hdac3KO macrophages
GSE98822 Hdac1Hdac2KO microglia P0 indCre
GSE54785 Hdac2KO colon
GSE50190 Hdac3KO IEC
GSE23700 Hdac2KO heart
GSE39946 Hdac1Hdac2KO lung
GSE85302 Kat6aKO CD8+Tcell
GSE90531 Hdac3KO islet
GSE10503 Hdac3KO liver P17
GSE98650 Hdac3KO Bcell
GSE74683 Elp3KO Forebrain
GSE47745 Hdac1Hdac2KO colon
GSE85929 Hdac3KO liver
GSE27451 Hdac1Hdac2KO Schwann
GSE98822 Hdac1Hdac2KO microglia E16 indCre
GSE98822 Hdac1Hdac2KO microglia P0 conCre
GSE66163 Hdac7KO proBcell
GSE101537 CrebbpKO islet
GSE10503 Hdac3KO liver P28
GSE98822 Hdac1Hdac2KO microglia 2wk conCre
GSE98822 Hdac1Hdac2KO microglia 6wk conCre
GSE56366 Hdac11KO macrophage
GSE101537 Ep300KO islet
GSE9134 Hdac5KO NucleusAccumbens
GSE98822 Hdac1Hdac2KO microglia 6wk indCre
GSE21087 Hdac3KO calvaria
GSE26488 Hdac7KO thymocytes
GSE94967 Ncoa2KO LiverTumor
GSE34229 Hdac6KO liver
-2.00
-1.33
-0.67
0.00
0.67
1.33
2.00
NES
Mouse brain 18m vs. 3m
Mouse brain 13m 50 mg/kg SAHA vs. DMSO
-1.00
-0.67
-0.33
0.00
0.33
0.67
1.00
z-score log2 FC

Fig. S5. KO of HATs and HDACs having similar (purple in up DEGs and green in down DEGs) or opposite (green in up DEGs and purple in down DEGs) gene expression patterns as aging or SAHA treatment.
(A) Heatmaps of GSEA NES (left) and z-score normalized $\log_2$ fold change (right) of HAT/HDAC knockout versus control gene expression changes in different mouse tissues from GEO database (5-30), compared with the effect of aging and SAHA in mouse brain.

Table S1. Human brain samples used in this study.
Information of human brain samples used for RNA-seq and ChIP-seq.

Group	Sample ID	Source	Age	Race	RIN
R 27 year old	200950	CBBC	24	Chinese	6.6
	2010336	CBBC	24	Chinese	7.6
	2009330	CBBC	25	Chinese	7.9
	2010150	CBBC	27	Chinese	6.3
	2010366	CBBC	27	Chinese	7.6
	2009193	CBBC	27	Chinese	8.2
	2008274	CBBC	29	Chinese	7.7
	2010177	CBBC	30	Chinese	7.8
	2010102	CBBC	32	Chinese	7.3
R 37.5 year old	777	CBBC	22	African American	7.3
	1026	CBBC	28	Caucasian	8.1
	1502	CBBC	29	Caucasian	7.4
	1326	CBBC	37	Caucasian	6.8
	816	CBBC	38	African American	7.3
	4645	CBBC	39	African American	7.9
	1375	CBBC	40	Caucasian	7.5
	871	CBBC	42	Caucasian	7.8
R 40 year old	2010321	CBBC	39	Chinese	6.3
	2008295	CBBC	40	Chinese	5.3
	2010056	CBBC	40	Chinese	6.5
	2008298	CBBC	40	Chinese	6.8
	2009290	CBBC	40	Chinese	8.1
	2010001	CBBC	41	Chinese	7
	2010324	CBBC	42	Chinese	5.1
	2010A	CBBC	42	Chinese	7
	2010024	CBBC	42	Chinese	7.6
R 56.5 year old	2011008	CBBC	54	Chinese	6.9
	2010016	CBBC	52	Chinese	7.1
	2010166	CBBC	60	Chinese	7
	2009114	CBBC	47	Chinese	7.4
	2009147	CBBC	47	Chinese	7.1
	2009337	CBBC	54	Chinese	6.9
	2008281	CBBC	59	Chinese	6.5
	2010022	CBBC	60	Chinese	6.7
	2009149	CBBC	52	Chinese	6.8
R 76.7 year old	34726040	ROSMAP	72.83	Caucasian	8.3
	92113025	ROSMAP	74.83	Caucasian	7.4
	21274866	ROSMAP	75.85	Caucasian	8
	36492755	ROSMAP	76.28	Caucasian	7.8

	10478041	ROSMAP	76.7	Caucasian	7.3
	15844425	ROSMAP	76.82	Caucasian	7.8
	67185070	ROSMAP	77.8	Caucasian	8.3
	10514454	ROSMAP	79.53	Caucasian	7.6
	50105437	ROSMAP	80.06	Caucasian	7.8
	11409232	ROSMAP	80.1	Caucasian	6.1
	21001933	ROSMAP	80.85	Caucasian	7
	10929637	ROSMAP	81.3	Caucasian	8.7
	50103967	ROSMAP	82.23	Caucasian	7.3
R 84 year old	20416210	ROSMAP	83.98	Caucasian	5
	61344957	ROSMAP	84.73	Caucasian	6
	24310553	ROSMAP	84.75	Caucasian	7.6
	20904509	ROSMAP	85.79	Caucasian	5.8
	95491648	ROSMAP	85.8	Caucasian	7.9
	53772202	ROSMAP	86.2	Caucasian	8.2
	20139850	ROSMAP	86.32	Caucasian	8.1
	50104422	ROSMAP	86.35	Caucasian	8.7
	20767628	ROSMAP	86.84	Caucasian	7.9
R 87.3 year old	20105242	ROSMAP	87.29	Caucasian	7
	44749170	ROSMAP	87.42	Caucasian	8
	89001223	ROSMAP	87.57	Caucasian	7.5
	10383017	ROSMAP	87.87	Caucasian	7.4
	11072071	ROSMAP	87.95	Caucasian	7.5
	22776575	ROSMAP	89.1	Caucasian	6.9
	91921829	ROSMAP	89.3	Caucasian	7.3
	50101659	ROSMAP	89.35	Caucasian	6.8
	50100482	ROSMAP	89.36	Caucasian	7.2
R 90.1 year old	11342432	ROSMAP	90.11	Caucasian	7.4
	70816595	ROSMAP	90.54	Caucasian	6.8
	50102376	ROSMAP	91.09	Caucasian	7
	87038802	ROSMAP	91.11	Caucasian	8.5
	67429065	ROSMAP	91.78	Caucasian	6.1
	41773404	ROSMAP	92.44	Caucasian	7
	82624422	ROSMAP	92.55	Caucasian	6.4
	89903942	ROSMAP	93.1	Caucasian	8.2
	50300084	ROSMAP	95	Caucasian	7.6
R 95.8 year old	23690880	ROSMAP	95.82	Caucasian	5.7
	21403733	ROSMAP	96.44	Caucasian	7.4
	50101523	ROSMAP	96.71	Caucasian	7.7
	43074402	ROSMAP	97.88	Caucasian	7.1
	20174533	ROSMAP	100.84	Caucasian	8.3
N 25 year old	2C0637	NICHD	24	Caucasian	5

	2C0607	NICHD	25	Caucasian	7
	2C0600	NICHD	25	Caucasian	5.1
	2C0625	NICHD	27	Caucasian	6.9
	2C0599	NICHD	27	Caucasian	5.7
N 33 year old	2C0630	NICHD	28	Caucasian	5.7
	2C0606	NICHD	32	Caucasian	5.5
	2C0615	NICHD	33	Caucasian	6.2
	2C0605	NICHD	34	Caucasian	6.4
	2C0622	NICHD	43	Caucasian	6.5
N 46 year old	2C0626	NICHD	46	Caucasian	7.6
	2C0618	NICHD	46	Caucasian	5.3
	2C0633	NICHD	46	Caucasian	5.2
	2C0627	NICHD	48	Caucasian	6.3
	2C0631	NICHD	48	Caucasian	5.3
N 64 year old	2C0621	NICHD	54	Caucasian	7.3
	2C0636	NICHD	59	Caucasian	5.9
	2C0638	NICHD	64	Caucasian	5.3
	2C0634	NICHD	67	Caucasian	6.3
	2C0635	NICHD	67	Caucasian	5.7

Table S2. Human brain Age-Up and Age-Down genes are enriched for different DNA binding proteins.
Using ChIP-seq data of DNA binding proteins in human cells are collected from ENCODE Databases, target enrichment for DNA binding proteins in the promoter (TSS +/- 1kp) or gene body (i.e. genes having ChIP-seq binding peaks by each of the DNA binding proteins) is tested against the rank list of genes sorted by their human brain expression RCC to age from high to low using GSEA. Top 20 enriched terms are shown. Proteins with NES>0 and <0 are consider as enriched among Age-Up and Age-Down genes, respectively.

Age-Up promoter

cell type	antibody	NES	FDR q-value
A549	Pol2(phosphoS2)	2.069	0.001
ECC1	GR	1.839	0.003
K562	EFOS	1.741	0.009
K562	BCL3	1.726	0.008
GM12878	p300	1.689	0.011
HeLa S3	BRG1	1.579	0.023
GM12878	EBF1	1.547	0.024
K562	FOSL1	1.529	0.024
GM12878	BCL3	1.500	0.026
GM18526	NFKB	1.474	0.028
H1-hESC	RXRA	1.467	0.028
Hep G2	HNF4A	1.461	0.027
A549	BCL3	1.456	0.027
ECC1	ERaa	1.440	0.028
Hep G2	HNF4	1.425	0.030
K562	HDAC6	1.424	0.029
Hep G2	RXRA	1.422	0.027
GM19193	NFKB	1.400	0.030
A549	FOSL2	1.397	0.030
K562	Pol2(phosphoS2)	1.386	0.032

Age-Up gene body

cell type	antibody	NES	FDR q-value
A549	Pol2(phosphoS2)	1.852	0.003
GM12878	Pol3	1.683	0.011
K562	Pol2(phosphoS2)	1.637	0.010
K562	BCL3	1.630	0.007
K562	HDAC6	1.621	0.006
Hep G2	ZBTB7A	1.478	0.018
K562	CTCFL	1.475	0.016
Hep G2	IRF3	1.462	0.015
HeLa S3	BRG1	1.448	0.015
K562	ZNF263	1.445	0.014
GM18526	NFKB	1.410	0.017

Hep G2	HNF4A	1.405	0.016
Hep G2	ERRa	1.397	0.016
K562	HDAC2	1.364	0.019
H1-hESC	RXRA	1.362	0.018
K562	ZBTB33	1.341	0.021
ECC-1	GR	1.337	0.020
GM12878	USF1	1.326	0.021
GM12878	NFYA	1.324	0.021
GM19193	NFKB	1.322	0.020

Age-Down promoter

cell type	antibody	NES	FDR q-value
SH-SY5Y	GATA3	-2.141	0.002
HMEC	EZH2	-1.761	0.023
PFSK-1	TAF1	-1.728	0.022
NHEK	EZH2	-1.692	0.022
HeLa S3	SPT20	-1.681	0.018
H1-hESC	CHD1	-1.622	0.025
HeLa S3	E2F1	-1.582	0.033
PFSK-1	SIN3A	-1.541	0.040
HeLa S3	TF3	-1.518	0.045
PFSK-1	NRSF	-1.513	0.042
HEK293	KAP1	-1.508	0.040
SH-SY5Y	GATA2	-1.501	0.038
SK-N-SH	NRSF	-1.472	0.044
K562	UBF	-1.471	0.041
HSMMT	EZH2	-1.467	0.040
Hep G2	NRSF	-1.444	0.045
HeLa S3	E2F1	-1.439	0.044
H1-hESC	YY1	-1.434	0.043
GM12878	YY1	-1.422	0.045
GM12878	NRF1	-1.422	0.043

Age-Down gene body

cell type	antibody	NES	FDR q-value
SH-SY5Y	GATA3	-2.350	0.000
HeLa S3	SPT20	-2.229	0.000
GM12878	ZNF274	-2.104	0.000
Hep G2	ZNF274	-2.076	0.000
IMR90	MAFK	-2.055	0.000
GM08714	ZNF274	-1.994	0.001
U2OS	SETDB1	-1.992	0.001
Hep G2	MAFF	-1.991	0.001
NT2D1	ZNF274	-1.979	0.001
K562	BRF2	-1.962	0.001
Hep G2	MAFK	-1.954	0.001

K562	MAFF	-1.920	0.001
HEK293	TCF7L2	-1.895	0.001
GM12878	JUND	-1.855	0.002
K562	MAFK	-1.805	0.002
H1-hESC	MAFK	-1.787	0.002
A549	FOXA1	-1.776	0.003
H1-hESC	CEBPB	-1.775	0.003
K562	KAP1	-1.774	0.002
HeLa S3	ZNF274	-1.758	0.002

Table S3. Mice used in this study.

Batch	Age (month)	Gender	Treatment	Mouse number	Mouse for RNA-seq	Mouse for ChIP-seq
1	3	Female	Blank	3	3	3
	18	Female	Blank	3	3	3
2	10	Female	Blank	12	6	3
	13	Female	DMSO	12	6	3
	13	Female	50 mg/kg SAHA	12	11	9
3	12	Male	DMSO	6	2	2
	12	Male	75 mg/kg SAHA	5	1	2
	12	Male	150 mg/kg SAHA	4	2	0

Table S4. KEGG pathways and NES values in the heatmap.
KEGG pathways have the same order as heatmap in Fig. 2A. Pathways enriched for Age-Up genes are mainly related to inflammation, while pathways enriched for Age-Down genes include neural specific functions and energy production metabolic functions in human brain. HDACi can globally reverse those age-related pathways.

KEGG pathways	Human brain ageing	Lu et al. 2004 ageing	CD4+ T cell TSA &Bu	HAEC TSA	HAEC SAHA	SK-N-SH SAHA	SK-N-Be(2)C SAHA
STAPHYLOCOCCUS AUREUS INFECTION	3.02	1.70	-2.04	1.62	1.51	-1.06	-1.07
INTESTINAL IMMUNE NETWORK FOR IGA PRODUCTION	2.62	1.33	-2.48	-1.11	-1.18	-1.10	-1.27
ALLOGRAFT REJECTION	2.59	1.66	-2.25	1.15	1.10	-1.47	-1.37
SYSTEMIC LUPUS ERYTHEMATOSUS	2.52	1.60	1.31	0.81	0.71	-0.87	-0.86
GRAFT-VERSUS-HOST DISEASE	2.45	1.62	-2.16	-0.90	0.82	-1.28	-1.30
AUTOIMMUNE THYROID DISEASE	2.44	1.63	-2.28	1.16	1.12	-1.32	-1.15
ASTHMA	2.39	1.67	-1.83	1.24	1.19	-1.23	-1.19
COMPLEMENT AND COAGULATION CASCADES	2.31	1.37	-1.46	0.96	-0.99	-0.93	-0.89
LEISHMANIASIS	2.26	1.06	-2.16	0.89	0.92	-0.90	-0.91
ANTIGEN PROCESSING AND PRESENTATION	2.26	0.99	-1.57	1.63	1.55	-0.92	-1.01
VIRAL MYOCARDITIS	2.23	1.16	-1.91	-1.41	-1.45	0.91	-0.96
MALARIA	2.19	1.63	-1.77	-0.96	-1.03	-1.12	-0.95
INFLAMMATORY BOWEL DISEASE (IBD)	2.19	1.10	-2.34	-1.30	-1.27	-1.04	-1.00
PHAGOSOME	2.16	0.97	-1.49	1.08	1.03	-1.26	-1.32
CYTOKINE-CYTOKINE RECEPTOR INTERACTION	2.14	1.01	-2.35	-1.42	-1.35	-0.95	-0.88
OSTEOCLAST DIFFERENTIATION	2.05	-1.15	-1.94	0.93	0.92	0.89	0.90
TYPE I DIABETES MELLITUS	2.03	0.86	-2.09	1.34	1.28	-1.19	-1.14
PERTUSSIS	2.00	-0.92	-1.73	-1.32	-1.30	0.75	0.86
RHEUMATOID ARTHRITIS	1.94	0.74	-1.65	0.99	0.93	-1.41	-1.39

CELL ADHESION MOLECULES (CAMS)	1.87	1.70	-2.11	1.28	1.28	-0.95	-0.97
NF-KAPPA B SIGNALING PATHWAY	1.87	1.24	-2.30	-1.22	-1.22	1.31	1.20
RIBOSOME	1.82	1.69	0.96	-2.06	-2.26	-2.11	-2.30
HEMATOPOIETIC CELL LINEAGE	1.78	0.84	-2.53	-1.08	-1.11	-1.39	-1.44
HERPES SIMPLEX INFECTION	1.77	1.09	-2.01	-1.41	-1.28	1.18	1.17
LYSOSOME	1.73	-0.90	0.95	1.41	1.34	-1.48	-1.60
LEUKOCYTE TRANSENDOTHELIAL MIGRATION	1.70	1.19	-1.87	0.91	-1.01	1.03	1.07
HTLV-I INFECTION	1.69	0.98	-1.59	-1.26	-1.29	1.25	1.26
TRANSCRIPTIONAL MISREGULATION IN CANCER	1.68	0.84	-1.55	-1.24	-1.12	1.17	1.12
VITAMIN DIGESTION AND ABSORPTION	1.68	0.47	0.93	-0.87	-0.95	0.80	-0.57
NOTCH SIGNALING PATHWAY	1.68	1.60	-0.97	-0.88	-0.87	1.19	1.25
BASAL CELL CARCINOMA	1.65	0.83	1.14	1.19	1.22	1.65	1.81
METABOLISM OF XENOBIOTICS BY CYTOCHROME P450	1.64	1.50	-0.96	1.15	1.08	-1.79	-1.67
NATURAL KILLER CELL MEDIATED CYTOTOXICITY	1.62	-1.28	-2.12	0.97	0.91	-1.28	-1.39
EPSTEIN-BARR VIRUS INFECTION	1.61	-1.15	-1.52	0.77	0.80	1.37	1.42
CYTOSOLIC DNA-SENSING PATHWAY	1.60	1.38	-1.88	-1.19	-1.26	-1.28	-1.33
TOXOPLASMOSIS	1.59	1.27	-1.57	1.02	0.95	0.83	0.94
TUBERCULOSIS	1.58	-1.25	-1.79	-0.87	-0.87	-0.91	-1.00
APOPTOSIS	1.58	0.82	-1.72	-1.35	-1.34	1.01	1.07
GLYCOSAMINOGLYCAN DEGRADATION	1.57	-0.95	-1.20	0.77	0.81	-1.12	-1.05
INFLUENZA A	1.56	-1.01	-1.87	-1.27	-1.36	-0.88	0.97
ECM-RECEPTOR INTERACTION	1.55	1.51	-1.14	1.02	1.01	-0.75	-0.73
FC GAMMA R-MEDIATED PHAGOCYTOSIS	1.54	-1.37	-1.44	-1.02	-1.07	1.36	1.47
PRIMARY IMMUNODEFICIENCY	1.52	0.76	-2.41	-0.71	-0.78	1.20	0.94

CHEMICAL CARCINOGENESIS	1.50	1.36	-1.06	1.02	0.96	-1.77	-1.65
JAK-STAT SIGNALING PATHWAY	1.50	0.97	-2.22	-1.07	-1.14	-0.90	-0.88
VIRAL CARCINOGENESIS	1.48	-1.15	-1.13	-1.17	-1.09	1.12	1.09
BASE EXCISION REPAIR	1.47	-0.75	-0.70	-1.61	-1.69	1.18	1.19
TYROSINE METABOLISM	1.47	1.21	1.04	0.63	0.57	1.44	1.60
PPAR SIGNALING PATHWAY	1.47	1.41	1.21	1.43	1.35	-1.07	-0.99
TNF SIGNALING PATHWAY	1.45	-1.01	-1.58	-1.01	-1.07	1.08	1.15
INSULIN RESISTANCE	1.45	-1.29	0.78	1.08	1.16	0.84	0.89
ADHERENS JUNCTION	1.44	0.73	-0.91	-1.13	-1.06	1.57	1.67
DRUG METABOLISM - CYTOCHROME P450	1.43	1.44	-1.32	0.86	0.83	-1.59	-1.48
PATHOGENIC ESCHERICHIA COLI INFECTION	1.42	-1.14	-1.22	-1.32	-1.40	1.27	1.14
MINERAL ABSORPTION	1.39	1.25	-0.82	1.89	1.91	-1.27	-1.30
MEASLES	1.38	1.39	-2.18	-1.22	-1.26	1.23	1.29
B CELL RECEPTOR SIGNALING PATHWAY	1.38	-1.56	-2.26	-0.96	-0.96	0.99	1.09
NOD-LIKE RECEPTOR SIGNALING PATHWAY	1.38	-1.09	-1.99	-1.39	-1.50	0.99	1.20
PRION DISEASES	1.37	-1.39	0.87	1.05	0.95	0.94	1.01
SALMONELLA INFECTION	1.33	-1.23	-1.24	-1.52	-1.51	1.31	1.42
CHAGAS DISEASE (AMERICAN TRYPANOSOMIASIS)	1.33	-1.09	-2.00	-1.28	-1.23	0.95	0.94
LEGIONELLOSIS	1.33	1.09	-1.50	-1.03	-0.99	-1.44	-1.33
GALACTOSE METABOLISM	1.31	-1.11	0.82	1.02	0.90	-1.14	-1.29
RAP1 SIGNALING PATHWAY	1.31	-1.54	-1.12	0.98	0.95	1.18	1.33
METABOLIC PATHWAYS	-1.18	0.90	1.07	1.12	1.07	-1.25	-1.31
DORSO-VENTRAL AXIS FORMATION	-1.19	-1.29	0.72	0.98	1.00	1.34	1.43
AMINOACYL-TRNA BIOSYNTHESIS	-1.19	-1.29	1.13	-1.41	-1.47	1.56	1.67
THYROID HORMONE SIGNALING PATHWAY	-1.19	-1.29	-1.14	0.92	0.93	1.42	1.48
RNA TRANSPORT	-1.20	-1.41	1.49	-1.23	-1.33	1.64	1.73
REGULATION OF	-1.20	1.24	-0.64	0.80	0.92	-0.78	-0.92

AUTOPHAGY							
GLIOMA	-1.21	-1.81	-0.94	-1.10	-1.03	-1.00	-1.11
PURINE METABOLISM	-1.23	-0.75	-0.85	-1.01	-1.06	1.12	1.12
LONGEVITY REGULATING PATHWAY	-1.23	-1.35	-0.68	-0.93	-0.88	1.01	1.04
PHOSPHOLIPASE D SIGNALING PATHWAY	-1.26	-1.64	-1.22	-1.01	-0.87	1.41	1.50
SYNAPTIC VESICLE CYCLE	-1.26	-2.27	1.92	1.91	1.96	-1.38	-1.39
LONGEVITY REGULATING PATHWAY - MULTIPLE SPECIES	-1.26	-1.17	-0.79	0.83	0.88	1.11	1.23
CHOLINE METABOLISM IN CANCER	-1.26	-1.78	-0.98	1.02	1.03	1.23	1.30
RENAL CELL CARCINOMA	-1.27	-1.63	-0.92	-0.96	-0.84	1.10	1.18
D-GLUTAMINE AND D-GLUTAMATE METABOLISM	-1.28	-1.08	0.87	-0.43	-0.45	1.11	1.16
FATTY ACID DEGRADATION	-1.28	1.80	0.89	1.19	1.14	-0.98	-0.91
ALANINE, ASPARTATE AND GLUTAMATE METABOLISM	-1.28	-1.13	1.21	1.49	1.34	1.28	1.43
RAS SIGNALING PATHWAY	-1.30	-1.64	-1.00	-1.06	-1.02	-0.91	-0.96
SPHINGOLIPID SIGNALING PATHWAY	-1.31	-1.26	-1.62	-1.01	-1.01	1.20	1.22
COLORECTAL CANCER	-1.31	-1.66	-1.51	-0.96	-0.95	1.16	1.33
WNT SIGNALING PATHWAY	-1.31	-0.98	-1.04	1.05	1.11	1.51	1.59
GASTRIC ACID SECRETION	-1.31	-1.54	-0.90	1.47	1.47	1.13	1.17
BIOSYNTHESIS OF UNSATURATED FATTY ACIDS	-1.32	0.70	0.93	-0.68	-0.84	0.96	1.09
NON-HOMOLOGOUS END-JOINING	-1.32	-1.45	-0.70	-1.27	-1.17	1.62	1.80
AMYOTROPHIC LATERAL SCLEROSIS (ALS)	-1.33	-1.51	-1.23	1.05	0.98	1.03	1.06
MELANOGENESIS	-1.33	-1.35	-1.05	1.31	1.28	1.52	1.66
CAMP SIGNALING PATHWAY	-1.34	-1.75	-0.96	1.16	1.26	1.22	1.33
FATTY ACID	-1.35	0.64	-0.89	1.06	1.01	0.99	0.97

BIOSYNTHESIS							
NEUROACTIVE LIGAND-RECEPTOR INTERACTION	-1.36	-1.76	-1.20	1.31	1.21	-0.94	-0.83
BETA-ALANINE METABOLISM	-1.36	1.36	1.08	1.31	1.28	-0.82	-0.94
ALDOSTERONE SYNTHESIS AND SECRETION	-1.38	-2.04	-0.91	1.42	1.42	1.13	1.14
VASOPRESSIN-REGULATED WATER REABSORPTION	-1.38	-1.16	-0.91	0.99	0.98	1.01	1.08
GAP JUNCTION	-1.38	-1.84	-1.04	0.88	0.84	1.49	1.41
NON-SMALL CELL LUNG CANCER	-1.38	-1.86	-0.97	-1.09	-1.05	1.04	1.02
GNRH SIGNALING PATHWAY	-1.43	-1.79	-0.99	-0.83	-0.81	1.35	1.28
PEROXISOME	-1.43	1.45	0.86	1.15	1.11	-0.91	-0.93
CIRCADIAN RHYTHM	-1.43	-0.99	-1.15	-1.30	-1.30	0.79	0.94
TERPENOID BACKBONE BIOSYNTHESIS	-1.44	-1.16	1.40	0.83	0.66	1.11	1.40
SEROTONERGIC SYNAPSE	-1.45	-1.47	-1.21	0.83	0.80	-1.19	-1.18
PROGESTERONE-MEDIATED OOCYTE MATURATION	-1.47	-1.99	-0.95	-1.25	-1.25	1.40	1.52
PROLACTIN SIGNALING PATHWAY	-1.49	-1.44	-1.05	-0.95	-0.94	1.39	1.50
PANCREATIC SECRETION	-1.49	-1.66	-1.13	1.43	1.44	-0.90	-1.00
INFLAMMATORY MEDIATOR REGULATION OF TRP CHANNELS	-1.49	-1.76	-1.62	1.00	0.94	0.89	0.98
AXON GUIDANCE	-1.50	-1.39	-0.85	1.20	1.20	1.09	1.07
PYRUVATE METABOLISM	-1.53	-1.12	0.49	0.82	0.77	0.92	1.05
VASCULAR SMOOTH MUSCLE CONTRACTION	-1.53	-1.35	-1.48	0.80	0.80	0.90	1.10
INOSITOL PHOSPHATE METABOLISM	-1.54	-0.91	-1.08	1.35	1.41	0.86	-0.97
FATTY ACID ELONGATION	-1.54	1.01	1.61	1.16	1.06	-1.41	-1.38
PANTOTHENATE AND COA BIOSYNTHESIS	-1.56	-0.56	-1.22	-1.06	-0.99	1.23	1.18

ERBB SIGNALING PATHWAY	-1.56	-2.13	-0.94	-1.04	-1.03	-0.90	-1.05
CALCIUM SIGNALING PATHWAY	-1.56	-1.90	-1.41	1.33	1.24	0.99	0.98
PHOSPHATIDYLINOSITOL SIGNALING SYSTEM	-1.58	-1.37	-0.97	1.39	1.47	-0.86	-1.01
CITRATE CYCLE (TCA CYCLE)	-1.60	-0.53	1.03	1.08	0.99	-0.89	-0.83
SALIVARY SECRETION	-1.61	-1.88	-1.66	1.51	1.59	0.83	0.90
ENDOCRINE AND OTHER FACTOR-REGULATED CALCIUM REABSORPTION	-1.64	-1.53	0.90	1.64	1.65	-0.85	-0.83
ADRENERGIC SIGNALING IN CARDIOMYOCYTES	-1.65	-1.58	-1.17	1.22	1.20	1.05	1.09
SELENOCOMPOUND METABOLISM	-1.66	0.89	1.04	-0.69	-0.64	1.14	1.36
RENIN SECRETION	-1.71	-0.78	-1.38	1.03	1.05	1.24	1.24
OXYTOCIN SIGNALING PATHWAY	-1.71	-2.00	-1.43	-0.96	-0.97	0.94	1.03
OOCYTE MEIOSIS	-1.73	-1.78	-0.75	-1.39	-1.38	1.56	1.58
CGMP-PKG SIGNALING PATHWAY	-1.77	-1.70	-0.86	1.14	1.18	1.36	1.44
LONG-TERM DEPRESSION	-1.79	-1.99	-1.24	0.86	0.83	1.13	1.23
MUCIN TYPE O-GLYCAN BIOSYNTHESIS	-1.80	-1.05	-1.02	0.74	0.85	-0.93	-0.81
AMPHETAMINE ADDICTION	-1.80	-1.92	0.83	1.54	1.52	1.48	1.53
CHOLINERGIC SYNAPSE	-1.81	-1.75	-1.18	1.44	1.39	0.89	0.97
PROPANOATE METABOLISM	-1.82	-1.13	1.17	1.20	1.12	-0.89	0.89
FATTY ACID METABOLISM	-1.90	1.23	1.23	1.06	1.01	1.00	1.13
SYNTHESIS AND DEGRADATION OF KETONE BODIES	-1.91	-1.58	-1.08	-1.08	-1.15	1.14	1.33
GLYCOSAMINOGLYCAN BIOSYNTHESIS - HEPARAN SULFATE AND HEPARIN	-1.93	-1.03	1.37	1.17	1.07	0.83	-0.97
CIRCADIAN ENTRAINMENT	-1.93	-1.93	-1.21	1.35	1.28	1.08	1.17
VALINE, LEUCINE AND	-1.95	1.43	1.21	1.32	1.26	-0.91	0.96

ISOLEUCINE DEGRADATION							
UBIQUITIN MEDIATED PROTEOLYSIS	-1.97	-1.32	-0.71	-1.52	-1.54	1.05	1.19
LONG-TERM POTENTIATION	-1.99	-2.34	-1.13	0.97	1.04	1.23	1.26
BUTANOATE METABOLISM	-2.04	-1.54	0.77	1.09	0.97	-0.81	-0.91
GLUTAMATERGIC SYNAPSE	-2.21	-2.20	-1.15	1.02	0.96	1.24	1.37
DOPAMINERGIC SYNAPSE	-2.29	-1.96	-1.03	1.35	1.32	1.33	1.40
NICOTINE ADDICTION	-2.30	-1.72	0.86	1.93	1.91	1.23	1.26
MORPHINE ADDICTION	-2.41	-1.99	-1.11	-1.01	-0.97	-0.84	-0.90
GABAERGIC SYNAPSE	-2.42	-1.89	0.82	1.06	0.99	-0.94	-1.11
RETROGRADE ENDOCANNABINOID SIGNALING	-2.43	-2.17	-0.94	1.18	1.06	0.87	0.86

References

1. Huang DW, Sherman BT, & Lempicki RA (2009) Systematic and integrative analysis of large gene lists using DAVID bioinformatics resources. *Nature Protocols* 4(1):44-57.
2. Huang DW, Sherman BT, & Lempicki RA (2009) Bioinformatics enrichment tools: paths toward the comprehensive functional analysis of large gene lists. *Nucleic Acids Res* 37(1):1-13.
3. Zhang Y*, et al.* (2008) Model-based analysis of ChIP-Seq (MACS). *Genome Biol* 9(9):R137.
4. Loven J*, et al.* (2013) Selective inhibition of tumor oncogenes by disruption of super-enhancers. *Cell* 153(2):320-334.
5. Whyte WA*, et al.* (2013) Master transcription factors and mediator establish super-enhancers at key cell identity genes. *Cell* 153(2):307-319.
6. Szklarczyk D*, et al.* (2017) The STRING database in 2017: quality-controlled protein-protein association networks, made broadly accessible. *Nucleic Acids Res* 45(D1):D362-D368.
7. Ashburner M*, et al.* (2000) Gene Ontology: tool for the unification of biology. *Nat Genet* 25(1):25-29.
8. Carbon S*, et al.* (2017) Expansion of the Gene Ontology knowledgebase and resources. *Nucleic Acids Res* 45(D1):D331-D338.
9. Weitzner DS, Engler-Chiurazzi EB, Kotilinek LA, Ashe KH, & Reed MN (2015) Morris Water Maze Test: Optimization for Mouse Strain and Testing Environment. *J Vis Exp* (100):e52706.
10. Wong CK*, et al.* (2018) The p300 and CBP Transcriptional Coactivators Are Required for beta-Cell and alpha-Cell Proliferation. *Diabetes* 67(3):412-422.
11. Knutson SK*, et al.* (2008) Liver-specific deletion of histone deacetylase 3 disrupts metabolic transcriptional networks. *EMBO J* 27(7):1017-1028.
12. Razidlo DF*, et al.* (2010) Histone deacetylase 3 depletion in osteo/chondroprogenitor cells decreases bone density and increases marrow fat. *PLoS One* 5(7):e11492.
13. Kraft M*, et al.* (2011) Disruption of the histone acetyltransferase MYST4 leads to a Noonan syndrome-like phenotype and hyperactivated MAPK signaling in humans and mice. *J Clin Invest* 121(9):3479-3491.
14. Trivedi CM*, et al.* (2010) Hopx and Hdac2 interact to modulate Gata4 acetylation and embryonic cardiac myocyte proliferation. *Dev Cell* 19(3):450-459.
15. Kasler HG*, et al.* (2011) Histone deacetylase 7 regulates cell survival and TCR signaling in CD4/CD8 double-positive thymocytes. *J Immunol* 186(8):4782-4793.
16. Jacob C*, et al.* (2011) HDAC1 and HDAC2 control the transcriptional program of myelination and the survival of Schwann cells. *Nat Neurosci* 14(4):429-436.
17. Chen X*, et al.* (2012) Requirement for the histone deacetylase Hdac3 for the inflammatory gene expression program in macrophages. *Proc Natl Acad Sci U S A* 109(42):E2865-2874.
18. Winkler R*, et al.* (2012) Histone deacetylase 6 (HDAC6) is an essential modifier of glucocorticoid-induced hepatic gluconeogenesis. *Diabetes* 61(2):513-523.

19. Ravnskjaer K, *et al.* (2013) Glucagon regulates gluconeogenesis through KAT2B- and WDR5-mediated epigenetic effects. *J Clin Invest* 123(10):4318-4328.
20. Turgeon N, *et al.* (2013) HDAC1 and HDAC2 restrain the intestinal inflammatory response by regulating intestinal epithelial cell differentiation. *PLoS One* 8(9):e73785.
21. Sun Z, *et al.* (2013) Deacetylase-independent function of HDAC3 in transcription and metabolism requires nuclear receptor corepressor. *Mol Cell* 52(6):769-782.
22. Alenghat T, *et al.* (2013) Histone deacetylase 3 coordinates commensal-bacteria-dependent intestinal homeostasis. *Nature* 504(7478):153-157.
23. Jamaladdin S, *et al.* (2014) Histone deacetylase (HDAC) 1 and 2 are essential for accurate cell division and the pluripotency of embryonic stem cells. *Proc Natl Acad Sci U S A* 111(27):9840-9845.
24. Stilling RM, *et al.* (2014) K-Lysine acetyltransferase 2a regulates a hippocampal gene expression network linked to memory formation. *EMBO J* 33(17):1912-1927.
25. Turgeon N, *et al.* (2014) The acetylome regulators Hdac1 and Hdac2 differently modulate intestinal epithelial cell dependent homeostatic responses in experimental colitis. *Am J Physiol Gastrointest Liver Physiol* 306(7):G594-605.
26. Crow M, *et al.* (2015) HDAC4 is required for inflammation-associated thermal hypersensitivity. *FASEB J* 29(8):3370-3378.
27. Azagra A, *et al.* (2016) In vivo conditional deletion of HDAC7 reveals its requirement to establish proper B lymphocyte identity and development. *J Exp Med* 213(12):2591-2601.
28. Laguesse S, *et al.* (2015) A Dynamic Unfolded Protein Response Contributes to the Control of Cortical Neurogenesis. *Dev Cell* 35(5):553-567.
29. Carpio LR, *et al.* (2016) Histone deacetylase 3 supports endochondral bone formation by controlling cytokine signaling and matrix remodeling. *Sci Signal* 9(440):ra79.
30. Newman DM, *et al.* (2016) Acetylation of the Cd8 Locus by KAT6A Determines Memory T Cell Diversity. *Cell Rep* 16(12):3311-3321.
31. Papazyan R, *et al.* (2016) Physiological Suppression of Lipotoxic Liver Damage by Complementary Actions of HDAC3 and SCAP/SREBP. *Cell metabolism* 24(6):863-874.
32. Remsberg JR, *et al.* (2017) Deletion of histone deacetylase 3 in adult beta cells improves glucose tolerance via increased insulin secretion. *Mol Metab* 6(1):30-37.
33. Renthal W, *et al.* (2007) Histone deacetylase 5 epigenetically controls behavioral adaptations to chronic emotional stimuli. *Neuron* 56(3):517-529.
34. Stengel KR, *et al.* (2017) Deacetylase activity of histone deacetylase 3 is required for productive VDJ recombination and B-cell development. *Proc Natl Acad Sci U S A* 114(32):8608-8613.
35. Datta M, *et al.* (2018) Histone Deacetylases 1 and 2 Regulate Microglia Function during Development, Homeostasis, and Neurodegeneration in a Context-Dependent Manner. *Immunity* 48(3):514-529 e516.